QUANTUM DOT LUMINESCENT SOLAR CONCENTRATOR: OPTIMIZATION OF CONCENTRATION AND THICKNESS

M. Rafiee*, S. Chandra, H. Ahmed and S. J. McCormack
Dept. of Civil, Structural and Environmental Engineering, Trinity College Dublin, Dublin 2, Ireland
* Corresponding author. Email: rafieem@tcd.ie Tel: +353 1 896 2671

ABSTRACT: The absorption coefficient of a Luminescent Solar Concentrator (LSC) can non-linearly affect the total optical efficiency (η_{opt}) and solar concentration ratio (C_P) of the device. Absorption is determined by two critical design parameters; the concentration of the luminescent material and the thickness of LSC plate. This paper presents a theoretical approach using a mathematical model based on a Ray Tracing algorithm to optimize these parameters to obtain the best LSC configuration design. A 60 × 60 × 3 mm LSC of CdSe/ZnS quantum dots (QDs) doped in epoxy resin was modelled and the model results were validated by comparing them to experimental results. To achieve the optimum thickness and luminescent material concentration of the LSC, a sensitivity analysis was carried out to predict the behavior of the LSC under different solar radiation. The LSC optical efficiency under standard AM1.5 global solar radiation was found to have reached a maximum (3.6%) at QD concentration of 0.55 wt%. Above this concentration, the optical efficiency was found to decrease due to re-absorption losses. Then, the thickness of the LSC was varied from 0.5 to 30 mm while the QD concentration was kept constant at the optimum (i.e. 0.55 wt%). Under these circumstances, the total optical efficiency has been observed to increase from 1.2% to 13.2% while the C_P was significantly decreased from 1.19 to 0.22 due to a decrease in the geometric gain.

Keywords: Luminescent Solar Concentrator, Ray Tracing, Modeling, Concentration, thickness, Quantum Dot, Emission, Absorption, Sensitivity Analysis

1 INTRODUCTION

Reducing spectral losses and enhancing efficiencies in Photovoltaic (PV) cells can be implemented by non-imaging optics based solar concentrating technology, such as LSC (Chatten et al., 2011, Chandra et al., 2012, S. Chandra, 2017). LSCs, illustrated in Fig. 1, consist of luminescent materials doped in a host material where the PV cell is attached to the edge of the device. As is seen, a portion of the solar radiation at the top surface is absorbed by the luminescent species and emitted at a single wavelength, where PV cells have higher efficiency. Then, through Total Internal Reflection (TIR), the emitted light is wave-guided to one of the LSC edges where the PV cell is located (Weber and Lambe, 1976, Goetzberger and Greube, 1977, Goetzberger, 1978). This improves the solar panel efficiency, as well as reducing the required PV area; thus, decreasing the final cost of the generated energy. LSC devices are able to convert and concentrate both diffuse and direct light; therefore, it is an adequate technology where diffuse solar radiation is dominant, such as in northern European countries where over 50% of light is diffuse (van Sark et al., 2008). They are low-cost and can be fabricated at small and large scales as transparent clear or coloured windows (Aste et al., 2015, Earp et al., 2004a). These features make them a preferred choice for use in Building Integration Photovoltaic (BIPV) systems and façades of buildings which brings us closer to the goal of constructing buildings with zero carbon energy consumption and buildings which are able to cover their required energy by renewable energies (Aste et al., 2011, Pagliaro et al., 2010, Debije and Verbunt, 2012). The absorption of LSC can non-linearly affect the performance and the total optical efficiency of the LSC device. From Beer Lambert law (Klampaftis et al., 2009, Şahin and Ilan, 2013, Abderrezek et al., 2013) absorbance is given as follows:

$$A = log_{10} T \quad (1)$$

Where T is the value of transmittance of LSCs. Absorbance is determined by two important design parameters; the concentrations of the luminescent material and the thickness of LSC plate.

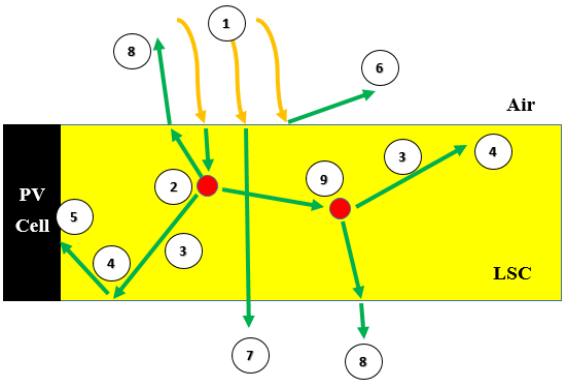

Figure 1: Configuration of LSC which shows: 1- solar ray is irradiated to the LSC, 2- absorbed by the luminescent material, then 3- re-emitted at longer wavelength and 4- wave-guided by Total Internal Reflection (TIR) and 5- reaches the PV cell. Losses include: 6- front surface reflection 7- the fraction of light which is lost through the bottom and 8- other surfaces (escape cone loss) and 9- the emitted light which is reabsorbed by another luminescent molecules and its energy is decreased

Modeling methods are required in order to design and optimize the LSC configuration. LSC mathematical models are implemented by either Thermodynamic or Ray Tracing methods (Batchelder et al., 1979, Carrascosa et al., 1983, Glassner, 1989, Barnham et al., 2000, Chatten et al., 2004, Earp et al., 2004b, Burgers et al., 2005, Kennedy et al., 2007, Kerrouche et al., 2014, Parel et al., 2015, Hughes et al., 2015). In a ray tracing model, each ray of light with specific wavelength and direction is traced until it leaves the system. The accuracy of both models were reported to be similar (Farrell et al., 2005) ; though, the ray tracing algorithm is more complex and time consuming in

comparison with thermodynamic model (Glassner, 1989). The advantage of ray tracing is that it is more flexible and can simulate different geometries and shapes of LSC with multiple luminescent species under diffuse and direct light (van Sark et al., 2008).

In this paper, LSC doped with CdSe/ZnS QD is modelled using a ray tracing algorithm. Modeling results were compared to experimental results to validate the ray tracing algorithm. Afterwards, a sensitivity analysis was undertaken to study and estimate the behavior of the LSC while changing the thickness of LSC and the QD concentrations under different solar radiation intensities. The modeling results were used to achieve the best and optimized configuration for the LSC.

2 RAY TRACING IMPLEMENTATION AND VALIDATION

The LSC ray tracing algorithm is based on a set of ray intersection calculation processes in an iterative loop due to the phenomena such as reflection, refraction, absorbing, scattering, attenuating and TIR events inside the LSC device. The process is continued till the fate of the ray is detected and then the same algorithm is executed for the other incident rays. The occurrence probability of each event at each stage of the ray tracing algorithm is determined according to parameters such as wavelength and angle of the incident ray, characteristics of the host and luminescent material, dimensions and configuration of the LSC. After implementing the iterative loop for all input rays, the optical efficiency of the LSC device is calculated by:

$$\eta_{opt} = \frac{\int_{\lambda_{min}}^{\lambda_{max}} E_{P_{OUT}}(\lambda).d(\lambda)}{\int_{\lambda_{min}}^{\lambda_{max}} E_{P_{IN}}(\lambda).d(\lambda)} \quad (2)$$

Where $E_{P_{OUT}}(\lambda)$ is the output energy spectrum detected at the edge of the LSC and $E_{P_{IN}}(\lambda)$ is the energy spectrum for the input solar radiation. Having known the optical efficiency of the LSC, the solar concentration ratio, C_P can be obtained by:

$$C_P = \Gamma \times \eta_{opt} \quad (3)$$

Where Γ is the geometric gain of the LSC and it is known as the aperture surface ratio (A_{APR}) to the total PV cell area (A_{PV}) which can be calculated as follows:

$$\Gamma = \frac{A_{APR}}{A_{PV}} \quad (4)$$

The ray tracing algorithm was used to model a 60 × 60 × 3 mm CdSe/ZnS QD LSC plate (Kennedy, 2010, Rowan, 2007, Kennedy et al., 2008, Kennedy et al., 2009) in which the PV solar cell was attached to one of its edges while the other edges have mirrors with reflectivity of ~1. The emission and absorption spectra of the LSC plate are shown in Fig.2.

The model was run for 100,000 input rays and the final results can be seen in Table I. Around 3.9% of the irradiated rays were reflected back from the top surface of the LSC device. The rest of the rays (96.1%) were refracted inside the LSC plate. Around 5.2% of rays were lost as heat inside the LSC which were either attenuated by the host material or absorbed by the QD and lost due to the non-unity quantum yield of the QD. Around 89% of the rays exited the LSC plate and were lost due the escape cone. Only a small portion of rays (~ 1%) were wave-guided to the edge of the LSC and detected by PV solar cell. The optical efficiency was calculated and found to be 1.6% which was in close agreement with the reference optical efficiency (1.63%).

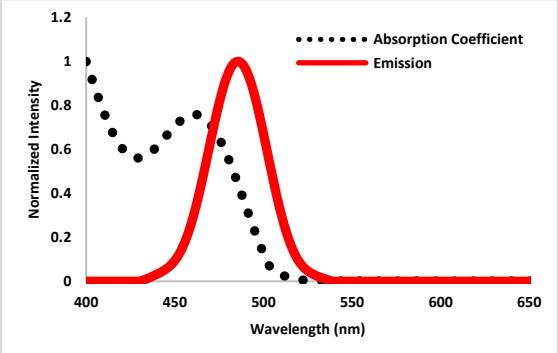

Figure 2: Normalized absorption coefficient and emission spectra for CdSe/ZnS QD LSC plate of 60×60×3 mm

Table I: Comparison and validation of the results obtained by the ray tracing model

Fate of the Rays	Value (%)
Reflected Light	3.90
Refracted Light	96.10
Lost Light	95.08
Light Reached PV	1.02
η_{opt} (REF=1.63% (Kennedy, 2010, Rowan, 2007, Kennedy et al., 2008, Kennedy et al., 2009))	1.6
C_P	32

3 SENSITIVE ANALYSIS AND DISCUSSION

In the second stage of the study, a sensitive analysis was undertaken to optimise the thickness of the QD LSC plate and the concentration of the QD under the standard AM1.5 solar radiation (Global, Direct and Diffuse). The QD concentration was varied from 0.1 to 1.2 wt% while the thickness of the LSC plate was 3 mm ($\Gamma = 20$). The modelling results are shown in Fig 3. Under global solar radiation, it has been observed that, the optical efficiency is linearly increasing as the QD concentration increased and reached its maximum (0.036) at concentrations between 0.55 - 0.6 wt%. Higher concentrations than 0.6 wt%, the optical efficiency is dropped and a saturation point is reached. The same trend was observed for the C_P as presented in Fig.3.b where it reached a maximum value of 0.7 and then started to decrease. The main reason for such behaviour is that by increasing the QD concentration, the re-absorption loss probability is increased. Moreover, by increasing the QD concentration, the emission peak was observed to be red-shifted. This is believed due to the fact that the photon loses some part of its energy in each re-absorption cycle. Fig 3.c shows the wavelength of the emission peak resulting from LSCs with different QD concentration values. As can be seen, for QD

concentration in the ranges of 0.1 to 0.3 wt%, the emission peak is red-shifted sharply from around 495 nm to 504 nm. It remains constant up to QD concertation of 0.5 wt% and then it is slightly increased again.

Under direct and diffuse solar radiation, the behaviour of the LSC has a similar trend to LSC under global radiation. The maximum η_{opt} and C_P for the LSC under diffuse solar radiation were respectively 0.043 and 0.86, at a QD concentration of 0.5 wt%. Under direct solar radiation, the η_{opt} and C_P were found to be 0.016 and 0.32, respectively at a QD concentration of 0.55 wt%.

The optimum QD concentration is therefore suggested to be between 0.5 - 0.6 wt% where the highest optical efficiency can be achieved under different solar radiation intensities.

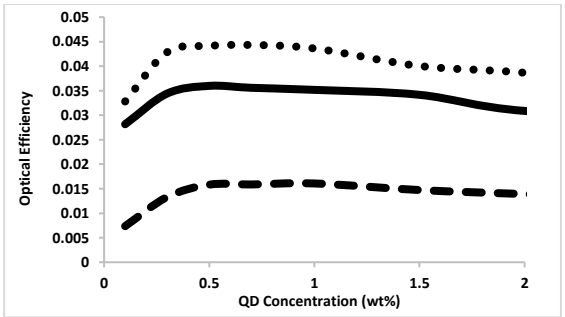

(a)

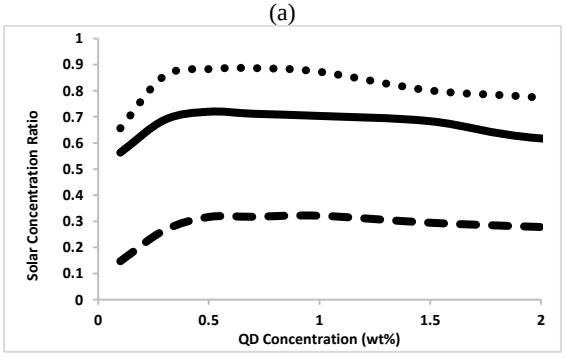

(b)

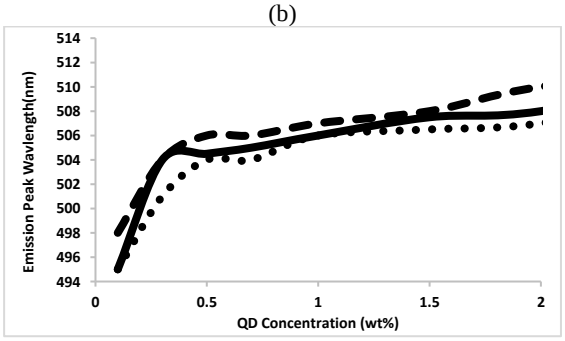

(c)

Figure 3: Modelling results under different solar radiations (Line: AM1.5 Global, Dash: AM1.5 Direct, Dots: AM1.5 Diffuse): (a) optical efficiency, (b) solar concentration ratio and (c) emission peak wavelength vs QD LSC concentrations

In the next step, the optimum concertation of the QD (0.55 wt%) was used to optimise the thickness, *d*, of the LSC plate in which *d* was varied from 0.5 to 30 mm while the value of QD concentration was kept constant. Fig.4 shows the optical efficiency for different LSC thicknesses.

It has been found that, the η_{opt} under global and diffuse solar radiation are in close agreement. The total optical efficiency increased non-linearly from around 0.01 to 0.13 for thicknesses between 0.5 to 30 mm. However, C_P is significantly decreased from around 1.7 to 0.5 for thicknesses between 0.5 to 5 mm and for thickness above 6 mm, C_P is slowly decreased to 0.22 (in thickness of 30 mm).

Under direct solar radiation, η_{opt} increased from 0.009 to 0.037 while the C_P decreased from 0.73 to 0.074.

This analysis shows that increasing the LSC thickness results in more light being detected at the edge of the LSC and increasing the optical efficiency; though, it reduces the geometric gain of the LSC which decreases the final solar concentration ratio, C_P.

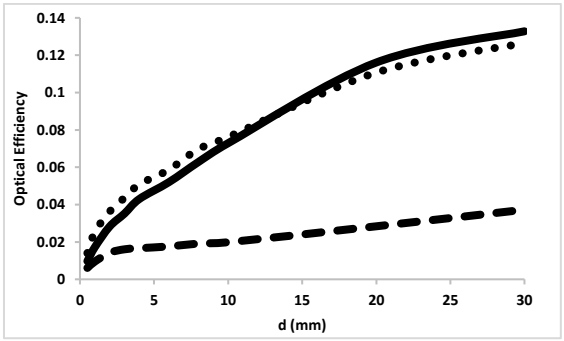

(a)

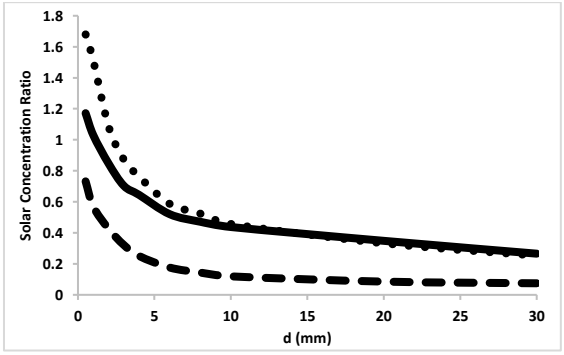

(b)

Figure 4: Modelling results under different solar radiations (Line: AM1.5 Global, Dash: AM1.5 Direct, Dots: AM1.5 Diffuse): (a) optical efficiency and (b) solar concentration ratio vs LSC thicknesses

4 CONCLUSION

In this paper, a ray tracing algorithm was used in order to model CdSe/ZnS QD LSC doped in epoxy resin polymer. The model was validated by comparing the simulation and measured results which were found to be in excellent agreement. Then, the validated model was used to study and predict the behavior of the LSC under different solar radiation intensities, LSC thicknesses and QD concentrations. The results showed that with QD concentration in the range of 0.5 - 0.6 wt%, the best η_{opt} and C_P can be obtained for the LSC plate under different solar radiation intensities investigated. It was found that, below a thickness of 6 mm the C_P was significantly increased due to the increase in geometric gain.

5 ACKNOWLEDGEMENT

The authors would like to acknowledge the funding from the European Research Council grant entitled PEDAL: Plasmonic enhancement of advanced luminescent solar devices (13379: 203889) and funding from Science Foundation Ireland (SFI). In addition, we also thank Dr. Manus Kennedy and Dr. Brenda Rowan whose thesis and research were used for validation of the model in this paper.

6 References

ABDERREZEK, M., FATHI, M., DJAHLI, F. & AYAD, M. 2013. Numerical Simulation of Luminescent Downshifting in Top Cell of Monolithic Tandem Solar Cells. *International Journal of Photoenergy*, 2013.

ASTE, N., ADHIKARI, R. & DEL PERO, C. Photovoltaic technology for renewable electricity production: Towards net zero energy buildings. Clean Electrical Power (ICCEP), 2011 International Conference on, 2011. IEEE, 446-450.

ASTE, N., TAGLIABUE, L. C., PALLADINO, P. & TESTA, D. 2015. Integration of a luminescent solar concentrator: Effects on daylight, correlated color temperature, illuminance level and color rendering index. *Solar Energy*, 114**,** 174-182.

BARNHAM, K., MARQUES, J. L., HASSARD, J. & O'BRIEN, P. 2000. Quantum-dot concentrator and thermodynamic model for the global redshift. *Applied Physics Letters*, 76**,** 1197-1199.

BATCHELDER, J., ZEWAI, A. & COLE, T. 1979. Luminescent solar concentrators. 1: Theory of operation and techniques for performance evaluation. *Applied Optics*, 18**,** 3090-3110.

BURGERS, A., SLOOFF, L., KINDERMAN, R. & VAN ROOSMALEN, J. Modelling of luminescent concentrators by ray-tracing. Presented at the 20th European Photovoltaic Solar Energy Conference and Exhibition, 2005. 10.

CARRASCOSA, M., UNAMUNO, S. & AGULLO-LOPEZ, F. 1983. Monte Carlo simulation of the performance of PMMA luminescent solar collectors. *Applied Optics*, 22**,** 3236-3241.

CHANDRA, S., DORAN, J., MCCORMACK, S., KENNEDY, M. & CHATTEN, A. 2012. Enhanced quantum dot emission for luminescent solar concentrators using plasmonic interaction. *Solar Energy Materials and Solar Cells*, 98**,** 385-390.

CHATTEN, A., BARNHAM, K., BUXTON, B., EKINS-DAUKES, N. & MALIK, M. 2004. Quantum dot solar concentrators. *Semiconductors*, 38**,** 909-917.

CHATTEN, A. J., FARRELL, D. J., BOSE, R., DIXON, A., POELKING, C., GÖDEL, K. C., MAZZER, M. & BARNHAM, K. W. Luminescent and geometric concentrators for building integrated photovoltaics. Photovoltaic Specialists Conference (PVSC), 2011 37th IEEE, 2011. IEEE, 000852-000857.

DEBIJE, M. G. & VERBUNT, P. P. 2012. Thirty years of luminescent solar concentrator research: solar energy for the built environment. *Advanced Energy Materials*, 2**,** 12-35.

EARP, A. A., SMITH, G. B., FRANKLIN, J. & SWIFT, P. 2004a. Optimisation of a three-colour luminescent solar concentrator daylighting system. *Solar Energy Materials and Solar Cells*, 84**,** 411-426.

EARP, A. A., SMITH, G. B., SWIFT, P. D. & FRANKLIN, J. 2004b. Maximising the light output of a Luminescent Solar Concentrator. *Solar Energy*, 76**,** 655-667.

FARRELL, D., CHATTEN, A., JERMYN, C., THOMAS, P. & BARNHAM, K. Thermodynamic Modelling of the Luminescent Solar Concentrator. INTERNATIONAL SOLAR ENERGY SOCIETY UK SECTION-CONFERENCE-C, 2005. 179.

GLASSNER, A. S. 1989. *An introduction to ray tracing*, Elsevier.

GOETZBERGER, A. 1978. Fluorescent solar energy collectors: operating conditions with diffuse light. *Applied physics*, 16**,** 399-404.

GOETZBERGER, A. & GREUBE, W. 1977. Solar energy conversion with fluorescent collectors. *Applied Physics*, 14**,** 123-139.

HUGHES, M. D., WANG, S.-Y., BORCA-TASCIUC, D.-A. & KAMINSKI, D. A. 2015. Analysis of ultra-thin crystalline silicon solar cells coupled to a luminescent solar concentrator. *Solar Energy*, 122**,** 667-677.

KENNEDY, M. 2010. *Monte-Carlo Ray-Trace Modelling of Quantum Dot Solar Concentrators.* PhD, Dublin Institute of Technology.

KENNEDY, M., MCCORMACK, S., DORAN, J. & NORTON, B. 2008. Ray-trace Modelling of Quantum Dot Solar Concentrators.

KENNEDY, M., MCCORMACK, S., DORAN, J. & NORTON, B. 2009. Improving the optical efficiency and concentration of a single-plate quantum dot solar concentrator using near infra-red emitting quantum dots. *Solar Energy*, 83**,** 978-981.

KENNEDY, M., ROWAN, B., MCCORMACK, S., DORAN, J. & NORTON, B. 2007. Ray-trace modelling of Quantum Dot Solar Concentrators and comparison with fabricated devices.

KERROUCHE, A., HARDY, D. A., ROSS, D. & RICHARDS, B. S. 2014. Luminescent solar concentrators: From experimental validation of 3D ray-tracing simulations to coloured stained-glass windows for BIPV. *Solar Energy Materials and Solar Cells*, 122**,** 99-106.

KLAMPAFTIS, E., ROSS, D., MCINTOSH, K. R. & RICHARDS, B. S. 2009. Enhancing the performance of solar cells via luminescent down-shifting of the incident spectrum: A review. *Solar Energy Materials and Solar Cells*, 93**,** 1182-1194.

PAGLIARO, M., CIRIMINNA, R. & PALMISANO, G. 2010. BIPV: merging the photovoltaic with the construction industry. *Progress in Photovoltaics: Research and Applications*, 18**,** 61-72.

PAREL, T. S., PISTOLAS, C., DANOS, L. & MARKVART, T. 2015. Modelling and experimental analysis of the angular distribution of the emitted light from the edge of luminescent

solar concentrators. *Optical Materials,* 42**,** 532-537.

ROWAN, B. 2007. The development of a quantum dot solar concentrator. *Doctoral***,** 12.

S. CHANDRA, H. A., M. RAFIEE AND S. J. MCCORMACK 2017. Plasmonic Quantum Dot Solar Concentrator. *SPIE Photonics West 2017*.

ŞAHIN, D. & ILAN, B. 2013. Radiative transport theory for light propagation in luminescent media. *JOSA A,* 30**,** 813-820.

VAN SARK, W. G., BARNHAM, K. W., SLOOFF, L. H., CHATTEN, A. J., BÜCHTEMANN, A., MEYER, A., MCCORMACK, S. J., KOOLE, R., FARRELL, D. J. & BOSE, R. 2008. Luminescent Solar Concentrators-A review of recent results. *Optics Express,* 16**,** 21773-21792.

WEBER, W. & LAMBE, J. 1976. Luminescent greenhouse collector for solar radiation. *Applied Optics,* 15**,** 2299.